1965

An instrument for the measurement of anelastic properties of glass

Thomas Frederick Miller

AN INSTRUMENT FOR THE MEASUREMENT OF ANELASTIC PROPERTIES OF GLASS

by

THOMAS F. MILLER

A

THESIS

submitted to the faculty of the

UNIVERSITY OF MISSOURI AT ROLLA

in partial fulfillment of the requirements for the

Degree of

MASTER OF SCIENCE, PHYSICS

Rolla, Missouri

1965

Approved by

D. E. Day (Advisor)

Louis N. Ramsay

R. O. Moore

Harold R. Fuller

ABSTRACT

An inverted torsion pendulum for measuring the internal friction and dynamic shear modulus of glass fibers over an extended temperature range has been constructed and calibrated. The calibration consists of the determination of the moment of inertia.

Extraneous damping losses were investigated and primary sources were found to be (1) the suspension thread, (2) the method of securing the fiber and (3) air damping.

Anelastic measurements were made on an annealed vitreous silica fiber and a soda-lime-silica fiber. The vitreous silica fiber was found to have a shear modulus of 3.21×10^{11} dy./cm.^{2} and an internal friction, or damping capacity, of 15.0×10^{-5}. The shear modulus of the soda-lime-silica glass was measured to be 3.00×10^{11} dy./cm.^{2} and the internal friction was found to be 500×10^{-5}.

ACKNOWLEDGEMENTS

The author is grateful to Dr. Delbert E. Day for the suggestion of the topic of this thesis and for his encouragement, direction and assistance throughout the course of this project. The author would also like to acknowledge the aid of Messrs. William Steinkamp and James Shelby.

The project was performed with the financial support of the Army Research Office-Durham, grant number DA-ARO-D-31-124-C550

The author would like to express his gratitude to Mrs. Patricia Miller who assisted with the format and typing of the thesis.

TABLE OF CONTENTS

Page

LIST OF FIGURES

LIST OF TABLES

I. INTRODUCTION

A. Introductory Remarks

Vitreous materials are unusual in the world of materials in that they exhibit properties of solids but have an internal structure similar to that of liquids. Many of the experimental techniques used to study the structure of crystalline materials provide only meager information about the structure of vitreous materials. This statement is supported by the difficulties encountered in studying the internal structure of vitreous materials. First, vitreous materials are in a nonequilibrium state, i.e., upon heat treatment practically all inorganic glasses revert to a lower energy state by nucleation and crystallization. However, at normal temperatures and over practical periods of time many glasses are quite stable with respect to crystallization. Second, glass is considered to be a solid incorporating the features of the liquid state such as short range order with no long range order. Features of the liquid state can be "frozen in" by rapid cooling from the melt. Since so many materials can be obtained as

glasses under certain conditions a great deal of effort has been made to develop techniques which can provide an understanding of the structural configurations capable of existing in vitreous materials.

As an example, internal friction studies of lithium silicate glasses[1] have demonstrated the ability of this technique to detect nucleation at earlier stages than X-ray diffraction and microscopic techniques. This technique, therefore, is one method of obtaining information about the early stages of crystal development.

B. Statement of Problem

The anelastic behavior of materials has been used to investigate the submicroscopic and short range structure of both crystalline and vitreous materials. This technique was first applied to metals and has been applied more recently to non-metallic and vitreous materials. This latter application is pertinent to the present work.

Torsion pendulums of various designs have been used to measure the absolute values of internal friction and the relative values of shear modulus, but have generally had limited versatility. Most of them have operated in air,

hence encountering viscous air damping, or have operated only over limited temperature intervals. Very few, if any, have been calibrated to yield absolute values of the shear modulus.

The value of internal friction measurements is the identification of loss mechanisms in a material which give rise to peaks in the internal damping versus temperature spectrum. To be useful, these peaks must be well resolved from the background damping. Relaxation mechanisms due to diffusion processes have a relaxation time τ governed by $\tau = \tau_o e^{\frac{\Delta H}{RT}}$ where ΔH is the activation energy, R is the universal gas constant, T is the temperature in degrees Kelvin, and τ_o is usually considered to be a constant for a particular material. For a periodic stress and strain of angular frequency ω Zener[2] shows the condition for maximum internal friction to be $\omega\tau=1$. Hence, measurements at high frequencies show damping peaks having lower relaxation times. That is, the effect of increasing the frequency is to shift the relaxation peak to higher temperatures. However, at higher temperatures the background damping of vitreous materials increases and the peak may become lost

in the background. When studying vitreous materials, therefore, it is advantageous to make measurements at low frequencies, about $\frac{1}{2}$ cps.

Most internal friction instruments used to study vitreous materials at a frequency of about 1 cps. have employed a simple torsion pendulum with the inertial element suspended by the sample which acts as the elastic member. Such an apparatus has an upper temperature limit determined by the transformation temperature of the glass fiber, since the fiber elongates under the weight of the inertial element at elevated temperatures. It should be possible to extend the upper temperature limit by using an inverted pendulum with the inertial element supported from above and the fiber clamped below, thus avoiding any tensile load on the fiber.

The primary objective of the present work was to design, construct, and calibrate an apparatus which avoided the limitations referred to above. It was desired to have the capability of determining the absolute shear modulus and of measuring the internal friction over as wide a temperature range as possible. To determine the absolute

value of the shear modulus by this technique, the moment of inertia of the pendulum must be accurately known. The determination of the moment of inertia, therefore, constituted a major portion of this study.

Two secondary objectives were (1) to obtain absolute values of the internal friction and shear modulus for vitreous silica and a typical soda-lime-silica glass, and (2) to investigate possible sources of energy loss other than those in the sample.

C. Literature Review

1. Theory of Internal Friction

Anelastic measurements have been used as a tool to study a wide variety of materials. Entwistle[3], Ke[4,5], and Klein[6] successfully applied this technique to metals, while McCrum[7] and Eby and Wilson[8] studied the internal friction and relaxation mechanisms in polymers. The theory found wide and successful application in the study of vitreous materials with the development of the torsion pendulum technique by Guye and Vasileff[9] for use at low frequencies.

Following the procedure used by De Mortin, Lott and Stainsby[10], simple damped harmonic motion in one dimension follows the equation of motion

$$\frac{d^2x}{dt^2} + 2\alpha\frac{dx}{dt} + \omega_o^2 x = 0 \qquad (1)$$

where ω_o is the natural angular frequency of oscillation without damping, 2α is the damping constant according to the assumed dissipative force relationship, $F = -2\alpha M\frac{dx}{dt}$, and M is the moment of inertia of the system. This equation has the complex solution

$$x = e^{-\alpha t}\,(Ae^{i\omega t} + Be^{-i\omega t}) \qquad (2)$$

where A and B are arbitrary constants and

$$\omega = \omega_o\sqrt{1-\frac{\alpha^2}{\omega_o^2}} \qquad (3)$$

or, in terms of real functions

$$x = Ae^{-\alpha t}\cos(\omega t + \delta) \qquad (4)$$

where the amplitude A and phase angle δ are determined by the initial conditions.

It is interesting to note that the damping is assumed linear with velocity. The same assumption is made by Zener[2] and can be shown to be true at least within

experimental accuracy by the linearity of the semi-logarithmic damping curve.

The amplitude envelope decreases as the exponential $e^{-\alpha t}$ and successive maxima are given by

$$x_n = x_o\, e^{-\alpha n P} \tag{5}$$

where n is the number of intervening cycles, and P is the period of one cycle. From this the logarithmic decrement, defined as

$$\delta = \alpha P = \frac{1}{n} \ln \left(\frac{x_o}{x_n}\right) \tag{6}$$

can be calculated. Zener[2] shows that the internal friction, tan δ, is related to the logarithmic decrement by $\tan \delta = \frac{\delta}{\pi}$. Tan δ is often referred to in the literature as Q^{-1} due to the straight-forward electrical analog. The ambiguous symbolism δ for logarithmic decrement and tan δ for internal friction will be eliminated by referring to internal friction as Q^{-1}.

2. Internal Friction of Vitreous Materials

The internal friction is related to the structure of the material through loss mechanisms. Sauer[11] classifies these as:

1. Thermoelastic damping due to stress gradient induced temperature gradients causing irreversible heat flow.

2. Stress induced diffusion occurring in solid solutions due to stress biasing of the normal diffusion process.

3. Slip at grain boundaries in polycrystalline materials.

4. Hysteresis or plastic flow damping arising essentially because the stress-strain curve is non-linear.

5. Damping by scattering of lattice waves which is significant only at very high frequencies in the megacycle region.

6. Viscoelastic damping which is analogous to viscosity losses in fluids.

In vitreous materials the loss mechanism of most interest is stress-induced diffusion. This source of energy lossgives rise to characteristic peaks in the temperature spectrum of the internal friction.

According to Zener[2], one advantage of scanning the temperature spectrum at constant frequency rather than

varying the frequency at constant temperatures is that an effective frequency range of three cycles of 10 will be traversed in raising the temperature from 0° to $60^{\circ}C$ when the heat of activation is 20 Kcal/mole. Thus, internal friction measurements extending over a temperature interval of several hundred degrees correspond to many decades of frequency. Varying the temperature is often easier than the experimental procedure required to cover the corresponding frequency interval.

The internal friction spectrum of alkali silicate glasses contains two peaks which rise considerably above the background. The low temperature peak, occuring at about $-30^{\circ}C$ at a frequency of about $\frac{1}{2}$ cps. has been attributed to the diffusion of the alkali ion[12,13,14]. There is controversy regarding the mechanism of the second peak which occurs at higher temperature. Forry[12] suggests that it may be due to the cooperative action of two coupled alkali ions. Douglas and Mohyuddin[14] favor the stress controlled movement of oxygen ions associated with only one SiO_4 tetrahedra, i.e., the diffusion of non-bridging oxygen ions.

By starting with a glass known to contain non-bridging oxygen ions and varying the composition in such a way that the number of such ions changed in a known manner, Day and Rindone[15] found a direct correlation between the number of non-bridging oxygen ions and the peak height. This correlation weighs heavily in favor of the stress controlled diffusion of the non-bridging oxygen ions as the loss mechanism of the second peak.

Some glasses exhibit a third, less prominent damping peak at approximately 300°C at $\frac{1}{2}$ cps. This peak has been less thoroughly studied. Day and Rindone[1] investigated this peak in a lithium silicate glass and found that its appearance and growth followed nucleation and crystallization, thus suggesting an interaction between the crystallites and the glassy matrix.

3. Techniques for Measuring Internal Friction

McCormick[16] describes an apparatus for the measurement of viscoelastic properties of glass utilizing an optical-electrical detection system. He describes two types of instruments, the first is a simple torsion pendulum suspended by the glass fiber and oscillating freely.

The second is a driven pendulum. The detection system consists of photocells, an electronic timer and a connecting scaling network. A spot of light reflected from a mirror on the moving element crosses the photocells and triggers the timer which measures the velocity of the pendulum at the equilibrium position. With this apparatus it is possible to measure the internal friction at frequencies of the order of 1 cps. with a precision of better than 10^{-4}. The frequency can be measured to within 0.02%. With this detection system the measured velocity is an average over the measuring interval and is something less than the true maximum instantaneous velocity. It is noted that with the measuring interval centered on the rest position and with an amplitude of at least three and one-half times the measuring interval, the average velocity measured is not less than 99.5% of the true velocity. The suggestion is made that the method of clamping the test samples is of extreme importance. McCormick also reports that in damping measurements air friction can introduce an error as large as the measurement itself in the case of vitreous silica.

At a pressure of 4 microns Hg, vitreous silica was reported to have a Q^{-1} of 19×10^{-5}

Blum[17] measured the internal friction of small diameter fibers of a typical soda-lime-silica glass using a simple suspended torsion pendulum. The purpose of this work was to determine if the surface condition affected the internal friction. The importance of viscous air damping was also investigated. The surface of glass fibers was damaged in a variety of ways and it was found that surface conditions other than gross flaws and severe water soaking had no effect on the damping. Under certain conditions air damping was observed to introduce errors of 10 to 50 per cent in the values for the internal friction. The magnitude of the torsional stresses and the fiber diameter were reported to have no effect upon the internal friction.

At 30°C the internal friction, Q^{-1}, for vitreous silica and for a typical soda-lime-silica glass was reported to be 1.3×10^{-5} (0.220 cps.) and 445×10^{-5} (0.350 cps.), respectively. The preceding value for the internal friction of vitreous silica is an order of magnitude less than that reported by McCormick.

An optical-electrical detection system is described in detail by De Morton, Lott and Stainsby[10]. The common method of measuring damping has been to follow optically the decay of amplitude by means of a light beam-optical lever-scale arrangement. This often laborious and time consuming technique has been improved by the utilization of an electronic detection system. It is reported that modulus changes can be measured to better than 1 in 10^4 with this system.

It has been reported by Blum[17], as well as in Zener's definitive work[2], that internal friction is independent of the torsional strain at low levels. Most experimental work, however, has been confined to simple suspended pendulums lacking any control over longitudinal stress in the fiber. In a recent study Klein[18] reported that the internal friction of chromium wires was dependent on both the applied torsional strain and the static tensile stress. The possibility of observing such behavior in glasses prompts the desire to incorporate control of these parameters into the equipment.

For fibers of low loss, ($Q^{-1} < 0.01$), extraneous energy damping in the system is often troublesome. While it is possible to perform internal friction measurements in air and correct for air damping, it is not particularly desirable. Douglas and Mohyuddin[14] used this approach by measuring the damping of vitreous silica in air and assuming the true internal friction to be 1×10^{-5}. The difference was attributed to air damping. However, in the equipment used by Douglas and Mohyuddin the internal friction of vitreous silica as measured in air was dependent upon both frequency and the ambient temperature. At a frequency of 0.152 cps. and at room temperature, a value of 17×10^{-5} was obtained for Q^{-1} in air. The air damping correction at this frequency and temperature was taken to be 16×10^{-5}. In this case the correction was sixteen times greater than the internal friction of vitreous silica.

The pendulum used by Douglas and Mohyuddin was of the simple or suspended type. It incorporated a rod projecting from the bottom which could be partially immersed in a cup of oil. The oil was assumed to damp transverse vibrations without significant damping of the torsional oscillations.

II. DESCRIPTION OF APPARATUS

A. General

For reasons discussed previously it was desired to use an inverted pendulum. The torsion member was suspended from a support by a thread which was assumed to have no rigidity and no loss. The validity of this assumption is discussed further in a later section. The restoring element or sample was in the form of a glass fiber approximately 70 millimeters in length and 0.6 millimeters in diameter. Figure 1 shows how the fiber is clamped in pin vises between the rigid base support and the torque rod. The pin vises had a 0.6 millimeter diameter hole drilled down the chuck, so that the jaws would close flush on a fiber of this diameter and permit very secure clamping without crushing the fiber.

The horizontal cross arms are fastened to a collar which slides along the vertical torque rod and which can be set at any desired position by a set screw. Figure 3 is a schematic diagram of the inertial member. The collar and the cross arms are of the same type steel and have the same density. The cross arms are threaded into the collar and

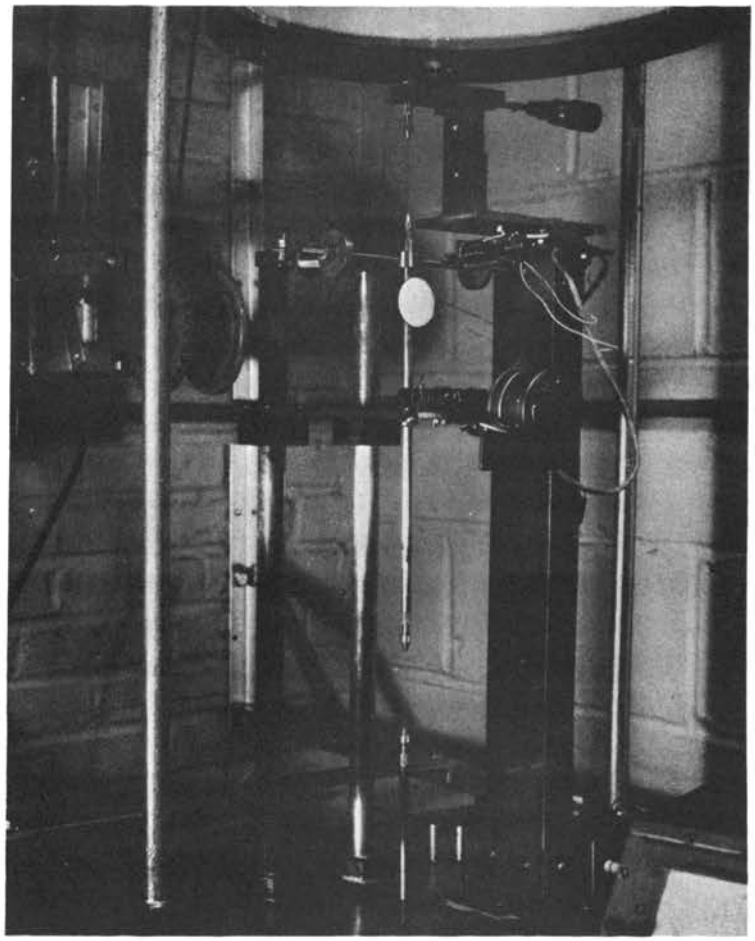

Figure 1. Torsion Pendulum

go through flush to the hole for the torque rod, leaving a solid cylinder of uniform density. These facts are employed in the calculation of the moment of inertia. The weights and weight locks are right circular cylinders, threaded to fit the cross arm. By changing the position of the weights, the moment of inertia can be varied from 2,400 to 15,000 $gm.cm^2$. This adjustment is used to maintain the frequency of oscillation within the range of 0.4 to 0.5 cps. The weight locks are tightened against the weights to insure that all rocking motion which might result in extraneous energy losses during oscillation are removed.

The inertial element is suspended from a counter weighted lever balanced on a knife edge. This construction allows for thermal expansion in the pendulum when it is placed in the furnace and maintains the tensile stress in the fiber at a constant value. By adjusting the position of the counter weight, the stress level can be varied from zero to a value close to that necessary for failure.

B. Temperature Control

The combination furnace-coolant chamber shown in Figure 2, consists of a hollow cylindrical core inside a

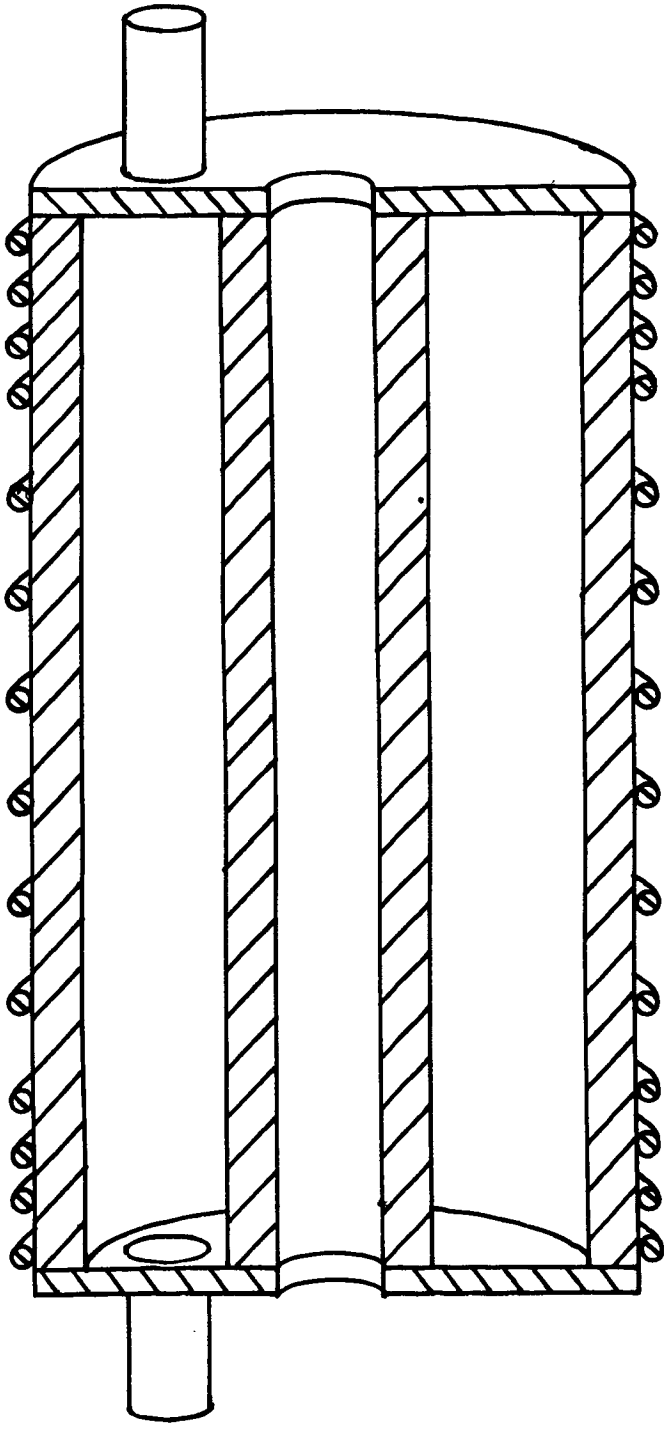

Figure 2. Furnace

larger cylinder. The ends are sealed with circular plates. At one end is an inlet tube, at the other an outlet tube. Construction is of stainless steel throughout. Coils of nichrome wire wrapped around the outer cylinder serve as resistance heating elements. Porcelain cement is used to insulate the heating coils from the stainless steel cylinder. About three inches of fiber insulation is placed around the entire assembly.

In operation, the glass fiber is axially and longitudinally centered in the hollow core. Liquid nitrogen is introduced into the annular chamber through the bottom inlet until the entire chamber is flooded, at which time the flow of liquid nitrogen is halted and a heating rate of about 2.5°C per minute is established using the heating coils. The temperature can be varied from -150°C to 900°C with a gradient of ± 1°C along the three inch region occupied by the sample. Any desired heating rate can be obtained by adjusting the powerstat which controls the electrical current in the heating coils.

The furnace slides vertically on support rods in order to afford access to the fiber. An iris diaphragm driven by

a servo motor is supported from the same rods. This diaphragm closes about the torque rod close enough to remove transverse vibrations without appreciably damping the torsional oscillations. It then opens sufficiently so as to not touch the oscillating parts while measurements are being made.

C. Air Damping

Viscous air friction is avoided by evacuation of the chamber to a pressure below ten microns Hg. Blum[17] has demonstrated that air friction is negligible at this pressure. The low frequency used also minimizes air damping. Douglas and Mohyuddin[14] found that for measurements made in air an air damping correction to Q^{-1} of 10×10^{-5} to 20×10^{-5} was required at a frequency of 0.152 cps. This value is peculiar to the equipment used in their work, but is indicative of the magnitude of the air damping.

D. Damping Measurements

The damping is obtained from the decay of the velocity rather than the amplitude decay. From equation (4), assuming an initial velocity of zero so that $\delta = 0$,

$$x = Ae^{-\alpha t}\cos\ \omega t, \tag{7}$$

from which the velocity can be obtained as

$$\dot{x} = \frac{dx}{dt} = Ae^{-\alpha t}(\omega\sin\omega t - \alpha\cos\omega t) \tag{8}$$

This function has maxima and minima at $\omega t = (n + \frac{1}{2})\pi$ and its damping envelope and frequency are identical to those of the amplitude. The logarithmic decrement can therefore be expressed as $\frac{1}{n} \ln \frac{\dot{x}_o}{\dot{x}_n}$.

Also:

$$Q^{-1} = \frac{\delta}{\pi} = \frac{\alpha P}{\pi} = \alpha\frac{2}{\omega} \tag{9}$$

so that

$$\dot{x} = A\omega e^{-\alpha t}(\sin\omega t - \tfrac{1}{2}Q^{-1}\cos\omega t). \tag{10}$$

The internal friction Q^{-1} is of the order 500×10^{-5} so it is a good approximation to drop the cosine term. The velocity can then be seen to be a damped sinusoidal curve, essentially the same as the amplitude.

The velocity is determined by measuring the time required for a light beam reflected from a mirror on the pendulum to traverse a distance of 1 centimeter. The light beam is focused by a concave mirror attached to the pendulum onto two parallel slits, 1 centimeter apart, which are centered at the rest position of the pendulum. As the

pendulum oscillates and the light beam sweeps back and forth across the slits, photo-sensitive cells behind the slits pulse a scaling network which starts and stops an electronic timer. Designating the time intervals corresponding to the zeroth and nth cycles as t_o and t_n respectively, the logarithmic decrement is given as $\frac{1}{n} \ln \frac{t_n}{t_o}$, and

$$Q^{-1} = \frac{1}{n\pi} \ln \frac{t_n}{t_o} \tag{11}$$

The scaling network was designed to register the time intervals for cycle intervals of one, two, four, eight, sixteen or thirty-two cycles. A period measurement can be made while the number of intervening cycles is being counted. The detector consists of a pick up containing the slits and photo-sensitive cells, amplifiers, a binary counting chain and a gating network. Solid state circuits are employed throughout, the circuitry is detailed in Appendix A.

Oscillation is initiated by symmetrically located electromagnets which furnish an initial angular displacement. Upon release, the pendulum vibrates at its natural angular frequency given by

$$\omega = \sqrt{\frac{\pi d^4 G}{32LI}} \tag{12}$$

where d, L and G are respectively the diameter, length and rigidity modulus of the fiber and I is the moment of inertia.

III. CALIBRATION OF APPARATUS

A. Theoretical Calculation of Moment of Inertia

The accurate calibration of the pendulum was an important aspect of this study since it was desired to measure simultaneously the absolute shear modulus and internal friction. There are few if any such values reported in the literature in the frequency range of 1 cps. This approach required the accurate determination of the moment of inertia of the torsion pendulum. A calculated value of the moment of inertia was obtained by using approximations to resolve any intractable integrations. An error analysis was performed to determine bounds on this value. Experiments were then devised to verify the calculated value within the error bounds.

The second moment of the mass, or the moment of inertia, about any axis can be calculated from the formula $I = \int r^2 \, dm$ where r is the normal radius vector from the axis to the element of mass and the integration extends over the entire mass. The moment of inertia of many complex systems can be found by dividing them into their

component sub-systems and taking advantage of any symmetry present.

To simplify the calculations, the inertial element of the torsion pendulum was divided into seven parts as shown in Figure 3. The moment of inertia of each part was calculated separately. The pin vises were further subdivided into seven parts as shown in Figure 4. Errors in dimensioning the pin vises were considered unimportant as the pin vises contribute less than one part in 2000 to the total inertia. The cross arm is threaded with 28 threads per inch. The moment of inertia of the system can be calculated as a function of the position of the weights with the position being expressed as the number of turns, n, from the innermost position. The moment of inertia of the off-axis parts was calculated by use of the parallel axis theorem which states that if the moment of inertia I of a rigid body of mass m is known about any axis through the center of gravity, the moment of inertia I' about any parallel axis removed a distance L is $I' = I + mL^2$.

Symmetry was maintained as closely as possible in order to achieve dynamic balance. Any departure from

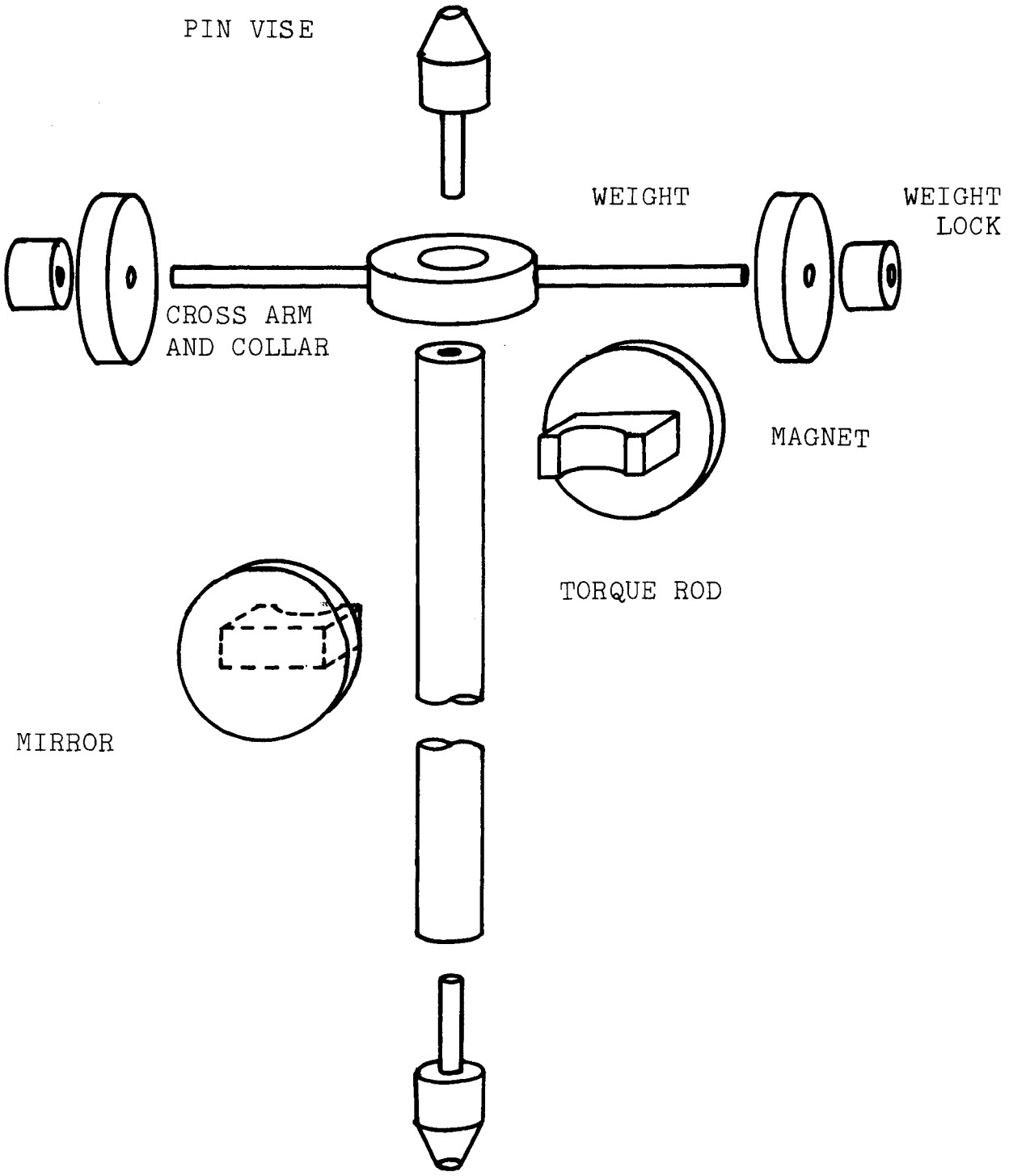

Figure 3. Inertial Member

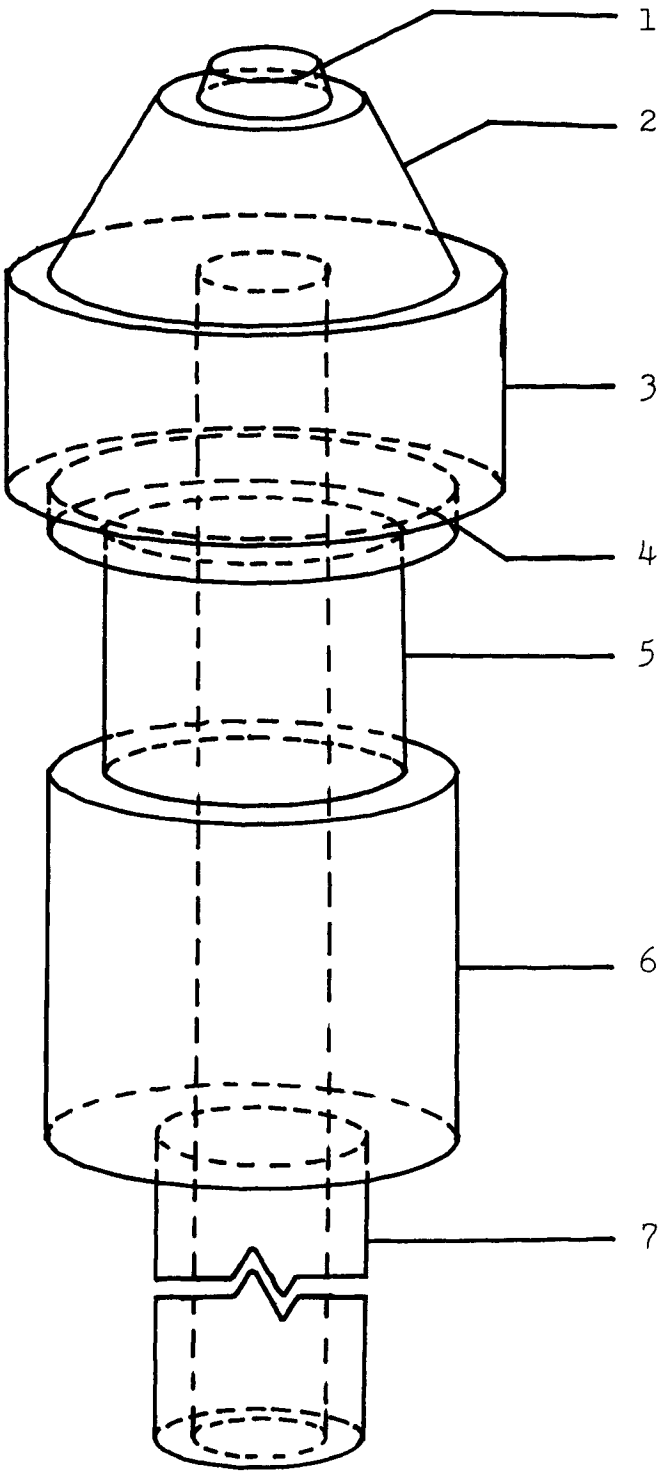

Figure 4. Pin Vise

symmetry would introduce coupling between normal vibrational modes, i.e., torsional and transverse. Such coupling has been maintained negligibly small.

Formulas used for calculating the moment of inertia for the component parts of the pendulum are listed below. A sample derivation of the moment of inertia formula for the magnet is given in Appendix B. Appendix C contains an error analysis yielding error bounds on I. Calculated values for the moments of inertia are listed in Table I, with values for the weights and weight locks being dependent on the first and second powers of n.

The moment of inertia formulae are:

Torque Rod,

$$I = \left(\frac{M}{2}\right)\frac{h_3 R_2^4 - (h_1 + h_2) R_1^4}{h^3 R_2^2 - (h_1 + h_2) R_1^2} \tag{13}$$

where

M = mass

R_1 = inside radius

R_2 = outside radius

h_1 = depth of top hole

TABLE I

Moments of Inertia

Component	I ($gm.cm^2$)
Torque rod	8.9
Cross arm and collar	1793.2
Magnet	7.3
Mirrors (2)	18.8
Weights (2)	216.0
Weight locks (2)	3.6
Pin vises (2)	1.1
Weight offset*	$383.2 + 40.52n + 1.095n^2$

*n = number of turns from innermost position

h_2 = depth of bottom hole

h_3 = length of rod

Cross Arm and Collar,

$$I = (\frac{M}{6})\frac{3h_1(R_2^4 - R_1^4) + h_2R_3^2(3R_3^2 + h_2^2 + 12(R_2 + \frac{1}{2}h_2)^2)}{h_1(R_2^2 - R_1^2) + 2R_3^2h_2} \qquad (14)$$

where

M = total mass

R_1 = inside radius of collar

R_2 = outside radius of collar

R_3 = radius of cross arm

h_1 = height of collar

h_2 = length of cross arm

Magnet,

$$I = M(\frac{A^2}{6} - \frac{R^4}{2}) \qquad (15)$$

where

M = mass

A = width

R = radius

Mirror,

$$I = \frac{M}{12}(3R^2 + h^2) \qquad (16)$$

where

M = mass

R = radius

h = thickness

Weight,

$$I = \frac{M}{2}(R_1^2 + R_2^2) \tag{17}$$

where

M = mass

R_1 = inside radius

R_2 = outside radius

Weight lock,

$$I = \frac{M}{2}(R_1^2 + R_2^2) \tag{18}$$

where

M = mass

R_1 = inside radius

R_2 = outside radius

Pin Vise,

$$I = \left(\frac{M}{4}\right)\frac{\frac{1}{10}\sum_{i=1}^{2} h_i \frac{b_i^5 - a_i^5}{b_i - a_i} + \frac{1}{2}\sum_{i=3}^{7} h_i (D_{2i}^4 - D_{1i}^4)}{\frac{1}{3}\sum_{i=1}^{2} h_i \frac{b_i^3 - a_i^3}{b_i - a_i} + \sum_{i=3}^{7} h_i (D_{2i}^2 - D_{1i}^2)} \tag{19}$$

where

M = mass

h_i = height of i^{th} conic or cylindric segment

$b_i (i=1,2)$ = base radius of i^{th} conic segment

$a_i (i=1,2)$ = top radius of i^{th} conic segment

$D_{1i} (i=3,..7)$ = inside diameter of i^{th} cylindric segment

$D_{2i} (i=3,..7)$ = outside diameter of i^{th} cylindric segment

From Table I the total moment of inertia in $gm.cm.^2$ is

$$I = 2430 + 40.5n + 1.10n^2. \qquad (20)$$

where n = number of turns from innermost position.

From Appendix C the error bound in $gm.cm.^2$ is

$$\Delta I = \pm (65 + 0.13n + 0.078n^2). \qquad (21)$$

The maximum percent error, $100(\Delta I/I)$, increases with increasing n. For $n = 90$, the largest possible value, the error is 4.7 per cent and for $n = 0$ the error is 2.7 per cent.

B. Experimental Verification

In the theoretical calculation of the moment of inertia, the complicated geometry of the components of the

pendulum made it necessary to make certain geometrical assumptions. While these assumptions were not considered to seriously affect the calculated value for the moment of inertia, it was considered desirable to determine an experimental value for the moment of inertia.

An experimental value for the moment of inertia can be determined from equation (12), when the period of the oscillation, the physical dimensions of the fiber, and the shear modulus, G, of the fiber are known. Since the period and the physical dimensions of the fiber can be measured, this leaves only the shear modulus to be determined. The static shear modulus of an annealed vitreous silica fiber was determined by applying known torques to the pendulum and measuring the angular displacement with the fiber clamped in the torsion pendulum. A graph of the torque versus angular displacement for the vitreous silica fiber is shown in Figure 5. The shear modulus of the fiber was calculated using the relationship

$$G = \frac{2LD}{R^4 \theta_D} \tag{22}$$

where

L = length of fiber

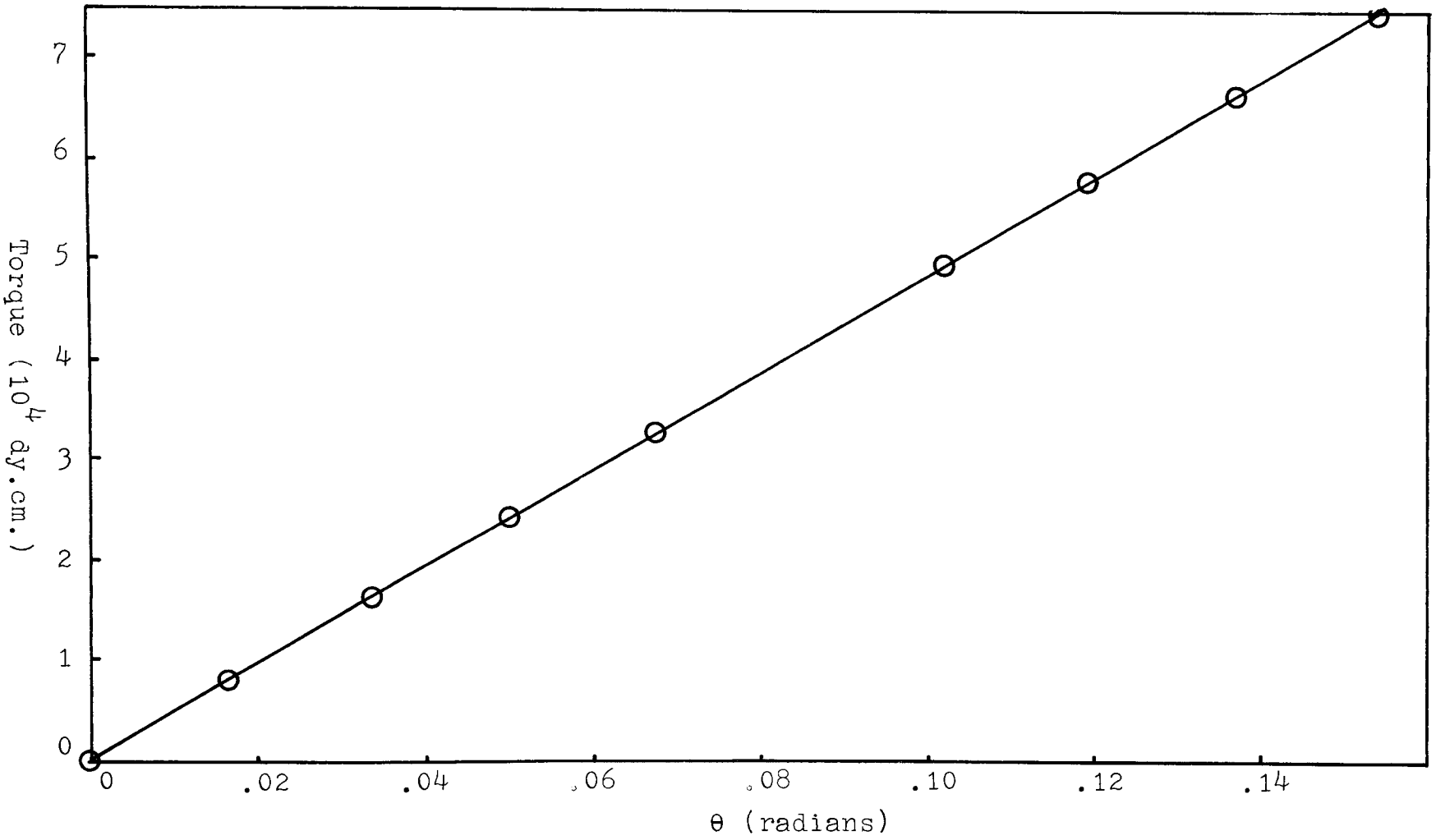

Figure 5. Torsional Stress-Strain

D = applied torque

R = radius of fiber

θ_D = angular displacement at torque D

After the static shear modulus had been determined the pendulum was set into oscillation and measurements of the period P were made. The moment of inertia was then calculated using equation (12).

The shear modulus of the vitreous silica fiber was calculated to be 3.21×10^{11} dy./cm^2. This value compares favorably with that reported by Horton[19] and Spinner[20]. They reported values for the shear modulus of 3.20×10^{11} and 3.15×10^{11} dy./cm.^{2}, respectively. The slight difference between the shear modulus determined in the present study and that reported by Horton and Spinner is attributed to the thorough annealing of the silica fiber used in this study.

With the weights set at the outermost position, n = 90 turns, the experimental value for the moment of inertia calculated from equation (12) was 15,060 gm.cm.^{2} The corresponding theoretical moment of inertia calculated from equation (20) is 14,980 gm.cm.^{2} the deviation between these

two values is 0.54 per cent.

Before measurements could be made with the weights in different positions, the vitreous silica fiber used for the initial measurement at n = 90 was broken. Another vitreous silica fiber was inserted in the pendulum. Without moving the weights, the shear modulus of the second fiber was calculated using equation (12) with the moment of inertia of 15,060 gm.cm.^{2} The weights were moved to positions corresponding to n equal 0, 30 and 60 turns, with period measurements taken at each position. The moment of inertia for each position of the weights was calculated from equation (12). The experimental values and the calculated values for the moments of inertia for the four positions of the weights are shown in Table II.

If the moment of inertia is plotted versus the square of the distance r from the vertical axis of the torque rod to the centroid of the weights, the parallel axis theorem predicts a linear relationship. This relationship is shown in Figure 6, where it is observed that the relationship is indeed linear. Values of r^2 are indicated corresponding to values of n of 0, 30, 60 and 90 turns. Note that n = 0 does not correspond to r = 0.

TABLE II

Theoretical and Experimental Values of Moment of Inertia

n (turns)	I Theoretical ($gm.cm^2$)	I Experimental ($gm.cm^2$)	Deviation
0	2,430	2,351	3.2%
30	4,635	4,573	1.3%
60	8,820	8,807	0.15%
90	14,980	15,060	0.54%

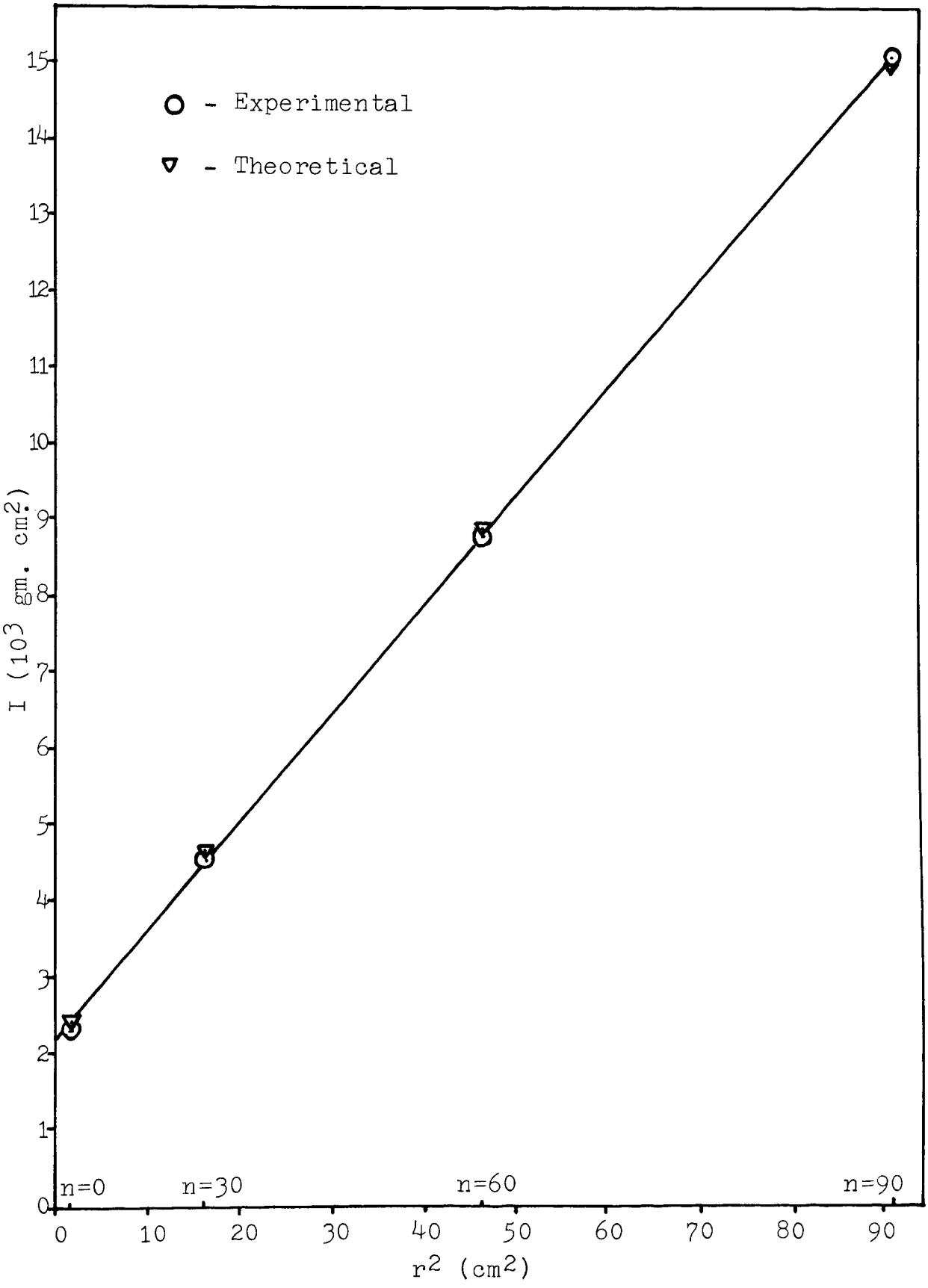

Figure 6. Moment of Inertia Vs. Position of Weight

IV. RESULTS AND DISCUSSION

A. Sources of Possible Extraneous Energy Loss

1. Suspension

The inertial element is suspended by a thread since it is desired to control the longitudinal stress in the fiber. This supporting thread has some small energy loss. To evaluate this contribution to the total damping, measurements were made on a vitreous silica fiber with the pendulum suspended first by the thread and then by the silica fiber. Supporting the pendulum by the fiber eliminates the thread from the system.

The internal friction of the vitreous silica fiber in air at atmospheric pressure was 37.9×10^{-5} and 34.0×10^{-5} with and without the thread, respectively. Values of Q^{-1} when measured in the inverted configuration, therefore, should be decreased by 3.9×10^{-5}. The contribution made by the thread to the total damping will be practically negligible, except for glasses of extremely low damping such as vitreous silica, when it is realized that the background damping of most glasses is in the range 100×10^{-5} to 300×10^{-5}.

2. Electromagnets

The use of electromagnets with soft iron cores could conceivably introduce an extraneous energy loss due to the cross arm moving in the inherent residual magnetic field. To evaluate this possible source of damping, measurements were made on a vitreous silica fiber in air, at atmospheric pressure with the magnets in place, and with the magnets removed. With the magnets removed, oscillation was initiated manually. Within experimental error, identical internal friction values were obtained, Figure 7.

A convenient means of displaying the damping data is to rearrange equation (11) as

$$\ln t_n = \pi Q^{-1} n + \ln t_o. \qquad (23)$$

A semi-logarithmic graph of t_n versus n is a straight line. Figure 7 shows the data used to check the effect of the electromagnets displayed in this manner. Extrapolation of the straight line to the initial and final values yields more accurate values for the internal friction than any two individual data points.

3. Grip Slippage

Any movement of the fiber in the pin vises constitutes

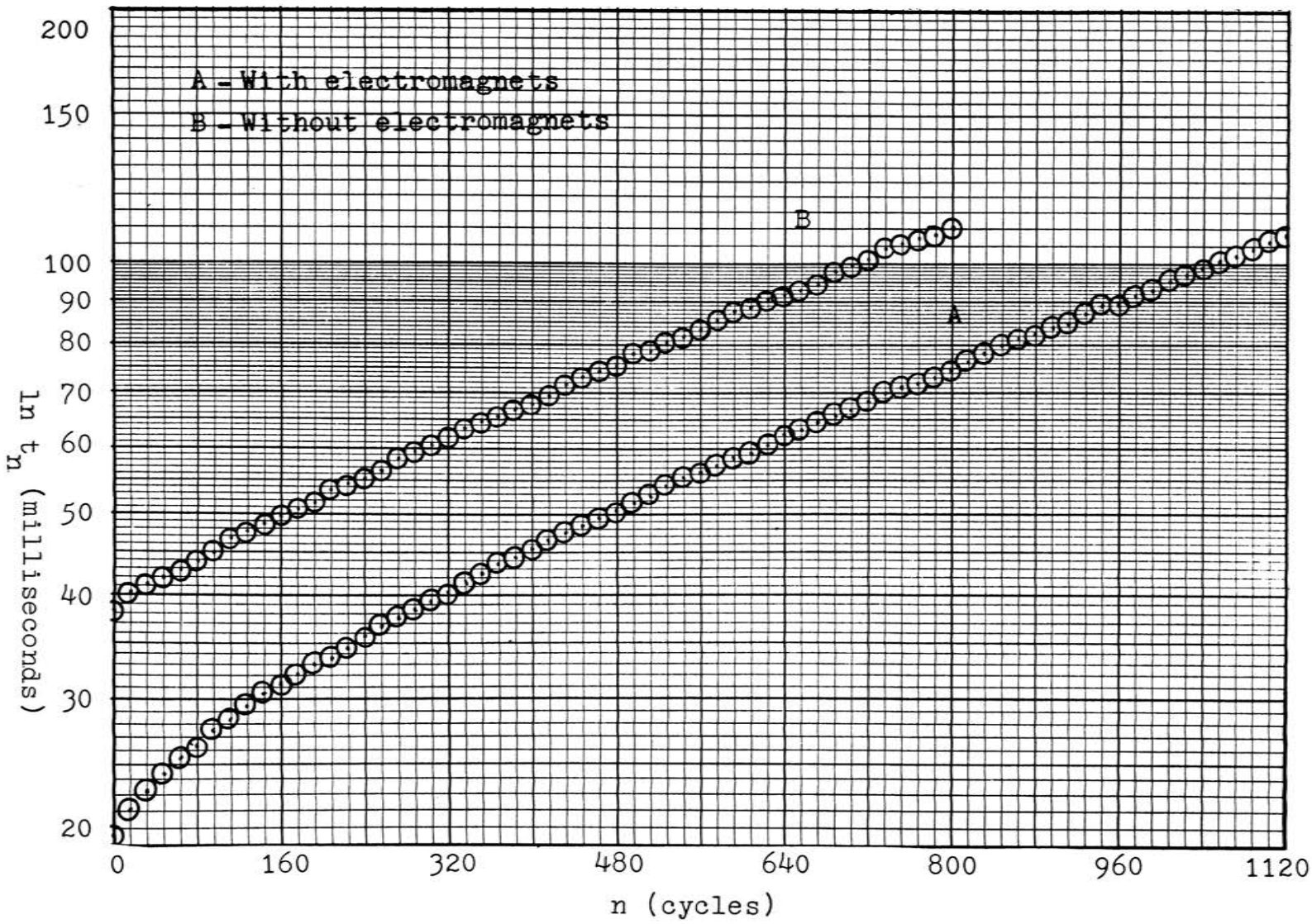

Figure 7. Damping Due to Electromagnets

a frictional energy loss with accompanying extraneous damping. McCormick[16] comments that the method of securing the fiber is of extreme importance. It was often possible to reduce the measured value for the internal friction of vitreous silica by tightening the pin vises with pliers. Untreated pin vises, i.e., those with the normal sharp gripping edges, could rarely be used to obtain low internal friction values since the fiber was often broken by the sharp gripping edges of the pin vises before the pin vises could be tightened adequately.

The damping data shown in Figure 7 for vitreous silica indicate that at large relative amplitudes, n less than 320, the internal friction is slightly higher than that observed at smaller amplitudes, n greater than 320. Since Q^{-1} is directly proportional to the slope of the curves shown in Figure 7, it is also apparent that at large relative amplitudes the damping is not constant, but varies slightly with the amplitude of vibration. This excessive damping at large amplitudes could result from either a minute slippage within the pin vises, or a slight amplitude dependence of the internal friction.

In metals the internal friction is commonly observed to be dependent upon the strain amplitude, i.e., the amplitude of vibration. However, in vitreous materials this behavior has not been reported. Thus, it is not known at the present time whether the internal friction of vitreous silica could also be slightly amplitude dependent.

Since a very small amount of slippage of the fiber within the pin vise could also account for this excessive energy loss at larger amplitudes, care must be taken to assure that the fiber is clamped securely. This dependency of the internal friction at larger amplitudes, while of academic interest, is not of practical importance to the present study since during a measurement the internal friction is always measured at amplitudes where the internal friction has assumed a constant value. However, an evaluation of different methods of clamping a fiber in the pendulum is indicated and should establish whether the use of pin vises is the best method which can be devised.

4. Air Damping

Internal friction measurements made in air on any

material are always subject to air damping. The magnitude of the air damping is primarily related to the design of the oscillating inertial member and can be reduced somewhat by designing this member for minimum viscous drag in air. Air damping is proportional to the square of the velocity and as such the damping is not strictly amplitude independent as has been assumed in the theory described previously. As a result of the dependence upon the square of the velocity, the correction for Q^{-1} is slightly amplitude dependent and is not a constant. However, if the correction for air damping is assumed to be a constant the error introduced is not large. In many investigations the internal friction values are not corrected for air damping, but in those studies where corrections for air damping are used the correction is taken to be a constant.

The magnitude of the air damping for the pendulum used in the present study was evaluated by measuring the internal friction of a vitreous silica fiber in air at atmospheric pressure and in a vacuum. The damping curves for vitreous silica at atmospheric pressure and at a pressure of less than 10 microns Hg are shown in Figure 8.

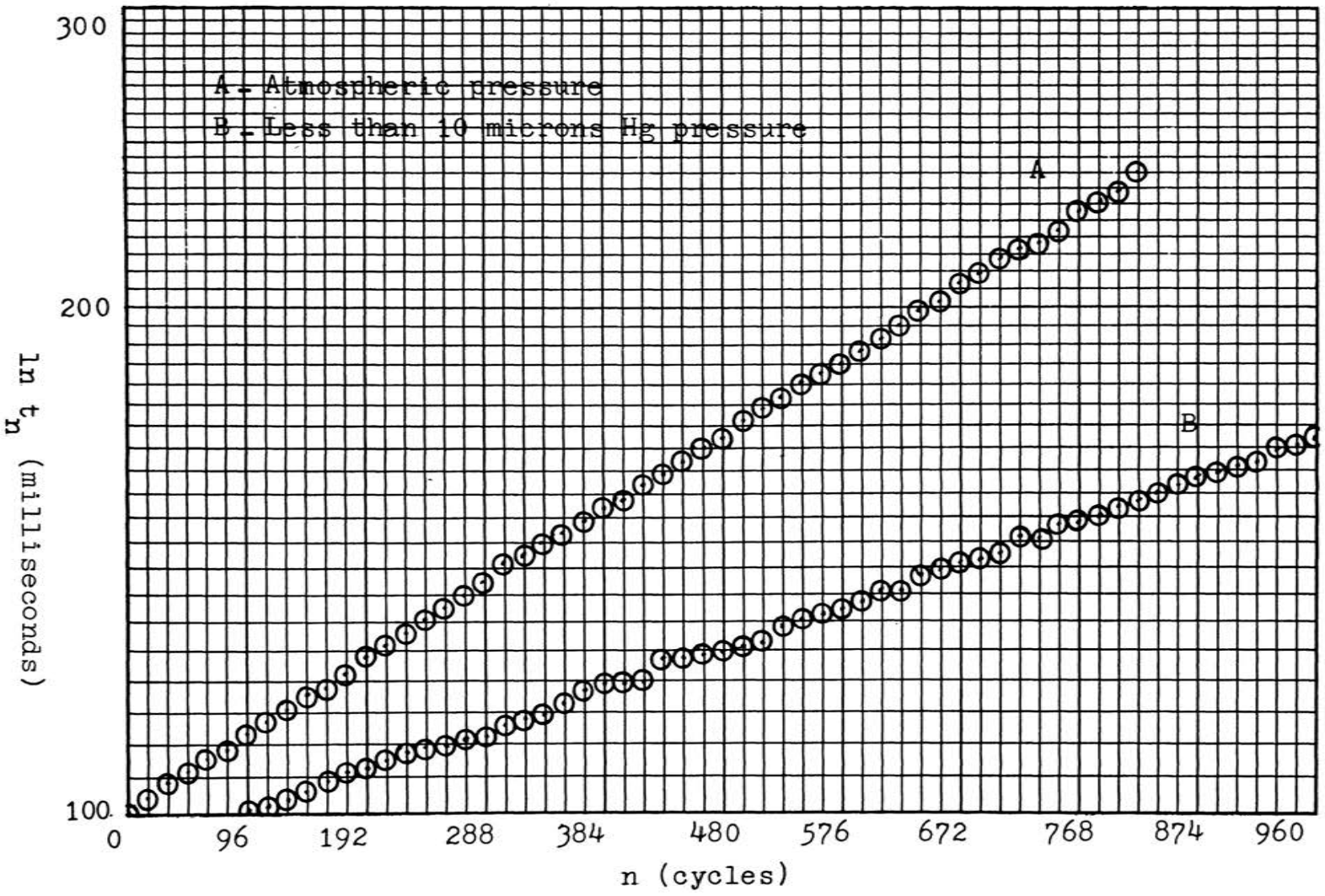

Figure 8. Air Damping

Under these two conditions the internal friction of vitreous silica was found to be 34×10^{-5} and 19×10^{-5}, respectively. The damping attributable to air friction, therefore, is 15×10^{-5}. Mohyuddin and Douglas[14] reported an air damping correction of 16×10^{-5} for their apparatus.

Obviously, a correction for air damping is necessary when it is desired to determine the true damping capacity of low energy loss materials such as vitreous silica. In many glasses, however, the internal friction is 300×10^{-5} to 1000×10^{-5} and in this case no serious error is introduced if the contribution form air damping is ignored.

B. Anelastic Measurements

1. Vitreous Silica

In comparison to other glasses, vitreous silica, has an extremely low absorption of energy. The internal friction is so low that accurate measurement is difficult. A value for Q^{-1} of 1.3×10^{-5} has been reported by Blum[17] for fibers 0.075 to 0.120 mm. in diameter. McCormick[16] reported a value of 19×10^{-5}. Horton[19] reported values of 13×10^{-5} and 1.3×10^{-5} under similar experimental

conditions with different instruments, after applying a correction for air damping.

In the present study the internal friction of an annealed vitreous silica fiber was found to be 19×10^{-5} at a pressure of less than 10 microns mercury. After correcting for the energy loss in the suspension thread, the internal friction becomes 15×10^{-5}. This value is in good agreement with that reported by McCormick[16] and with one of the values reported by Horton[19].

2. Soda-Lime-Silica Glass

The internal friction of this glass was determined using fibers 0.5 - 1.0 mm. in diameter which had been drawn from a heated portion of a rod approximately 10 mm. in diameter. This glass has an approximate composition of 74% SiO_2, 14% $Na_2O + K_2O$, 11% CaO, and 1% Al_2O_3. The fibers were not annealed after drawing.

Static measurements yielded a shear modulus of 2.97×10^{11} dy./cm.^{2} whereas dynamic measurements at $\frac{1}{2}$ cps. yielded a shear modulus of 3.08×10^{11} dy./cm.^{2} The internal friction at 23°C, $\frac{1}{2}$ cps. and less than 10 microns Hg was found to be 500×10^{-5}. Blum[17] reported a value of 450×10^{-5}

for chilled soda-lime-glass under nearly identical experimental conditions. It should be noted that the internal friction of the soda-lime-silica glass is approximately 30 times that of vitreous silica.

V. SUMMARY

An instrument for measuring the internal friction and dynamic shear modulus of a material has been designed, constructed and calibrated. With this equipment the internal friction can be measured over the temperature range 78 to 1270°K and at frequencies of 0.1 to approximately 10 cycles per second. The pressure can be varied from atmospheric to less than three microns mercury.

The calibration of the instrument included (1) an accurate determination of the moment of inertia of the oscillating member and (2) an evaluation of possible sources of extraneous energy loss within the instrument.

The moment of inertia was initially calculated from the geometry of the inertial components and then verified experimentally. Agreement between the two methods was within two per cent. From this agreement it is concluded that the theoretical equation

$$I = 2430 + 40.5n + 1.10n^2$$

can be used in the determination of the dynamic shear modulus of experimental glass fibers. The error in the

shear modulus should be no more than 3% when all of the variables used in evaluating this property are considered.

Three possible sources of extraneous energy loss were identified. These are (1) the thread from which the inertial member is suspended, (2) slippage within the pin vises, and (3) air friction. The internal friction of the thread was found to be 4×10^{-5}. This correction is so small that it can generally be ignored except for materials of extremely low energy absorption such as vitreous silica. The energy loss resulting from the slippage of the fiber within the pin vises could not be completely determined. This energy loss while of some importance at large amplitudes is negligible at amplitudes over which the internal friction of a glass fiber will be measured. The energy loss due to air friction was determined to be 15×10^{-5}. This correction can also be ignored without serious error for most glasses.

Measurements of the internal friction of vitreous silica and a soda-lime-silica were made to check the overall operation of the torsion pendulum. In both glasses, the internal friction values obtained with this apparatus

were in good agreement with those reported in the literature.

The precision of the internal friction measurements is demonstrated by the smoothness and linearity of the semi-logarithmic (damping) curves. Consecutive, identical measurements have indicated that the internal friction values have a precision of ± 0.2 per cent. The frequency (or period) of the pendulum can be measured within 0.1 per cent.

VI. APPENDICES

APPENDIX A

Circuitry of Detection System

The detection system consists of five basic circuits arranged as a scaling network. Figures 9, 10, 11, 12 and 12 show these basic circuits. Figure 14 shows their interconnection.

As shown in Figure 12, pulses are channeled to the binary counting chain until the desired number is reached, at which time the flip-flops are all reset to zero. This is the only configuration in which the first AND gate opens. During the next sweep of the light beam the second AND gate opens and pulses proceed from the inverters to the timer.

The output of the flip-flops is always near zero or minus ten volts. Nothing approaching a half-way voltage should be registered.

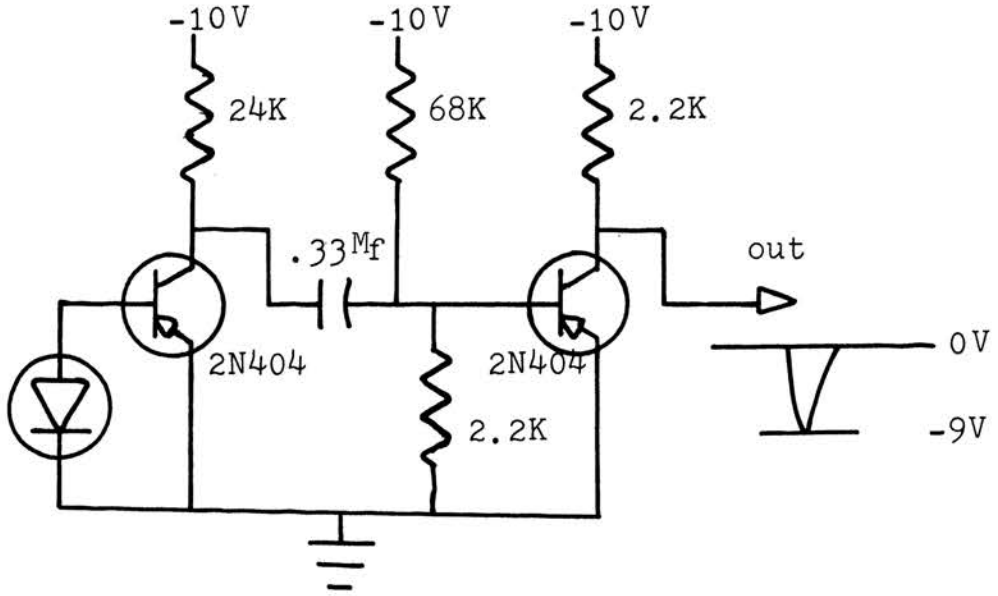

Figure 9. Pickup and Amplifier

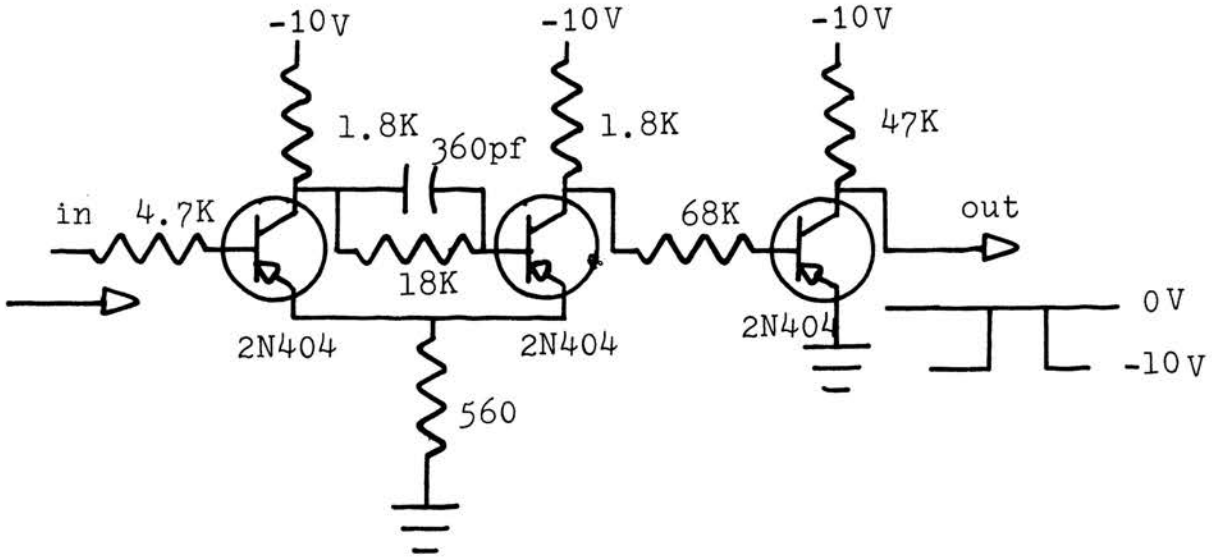

Figure 10. Pulse Shaper and Inverter

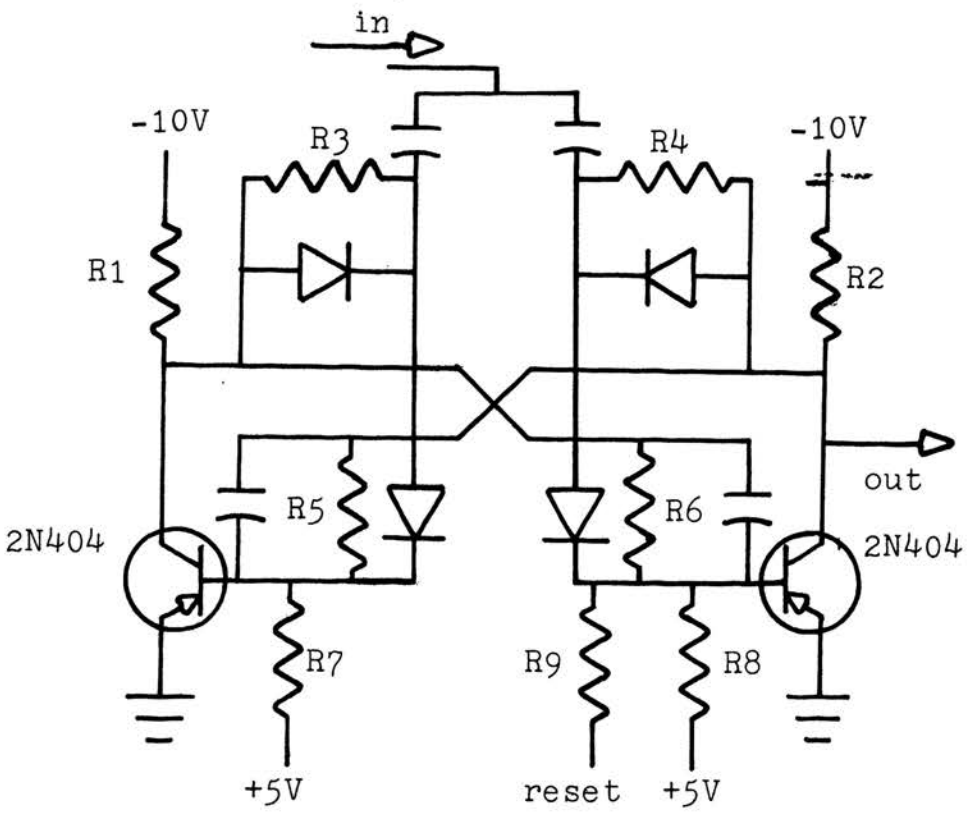

R1,R2	2.2K,0.5W,10%
R3,R4	18K,0.5W,10%
R5,R6	10K,0.5W,10%
R7,R8	68K,0.5W,10%
R9	18K,0.5W,10%
All Capacitors	360pf
All Transistors	2N404
All Diodes	TI53

Figure 11. Binary Flip-Flop

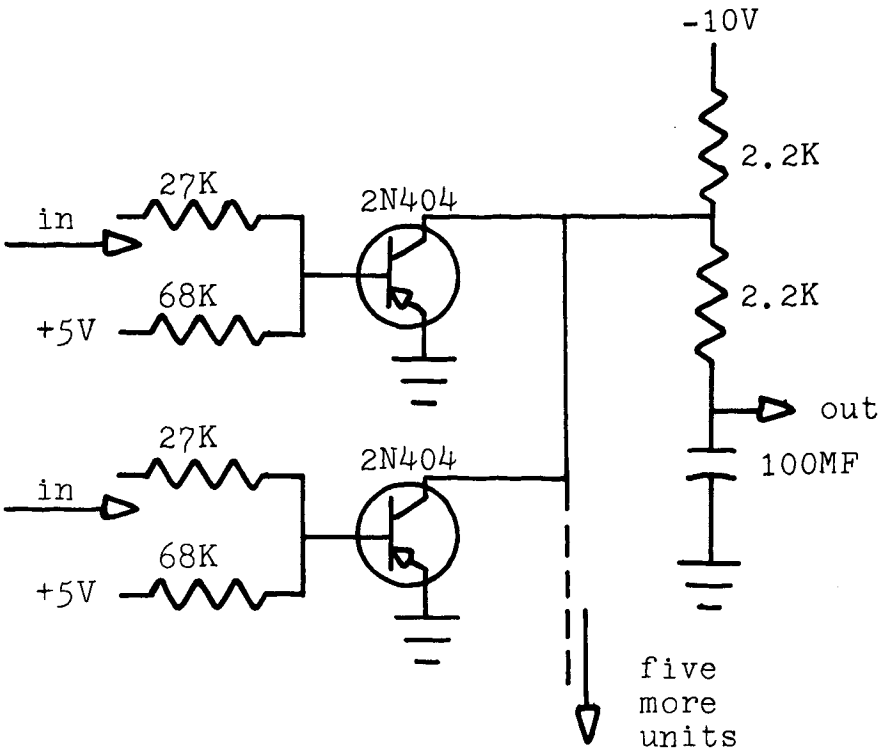

Figure 12. First AND Gate

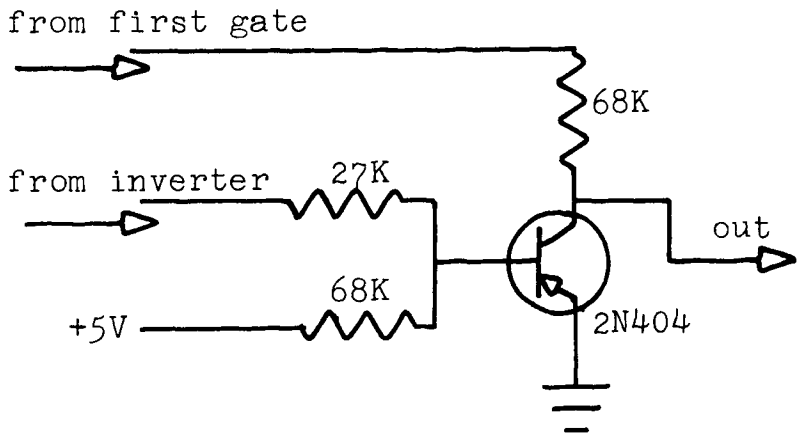

Figure 13. Second AND Gate

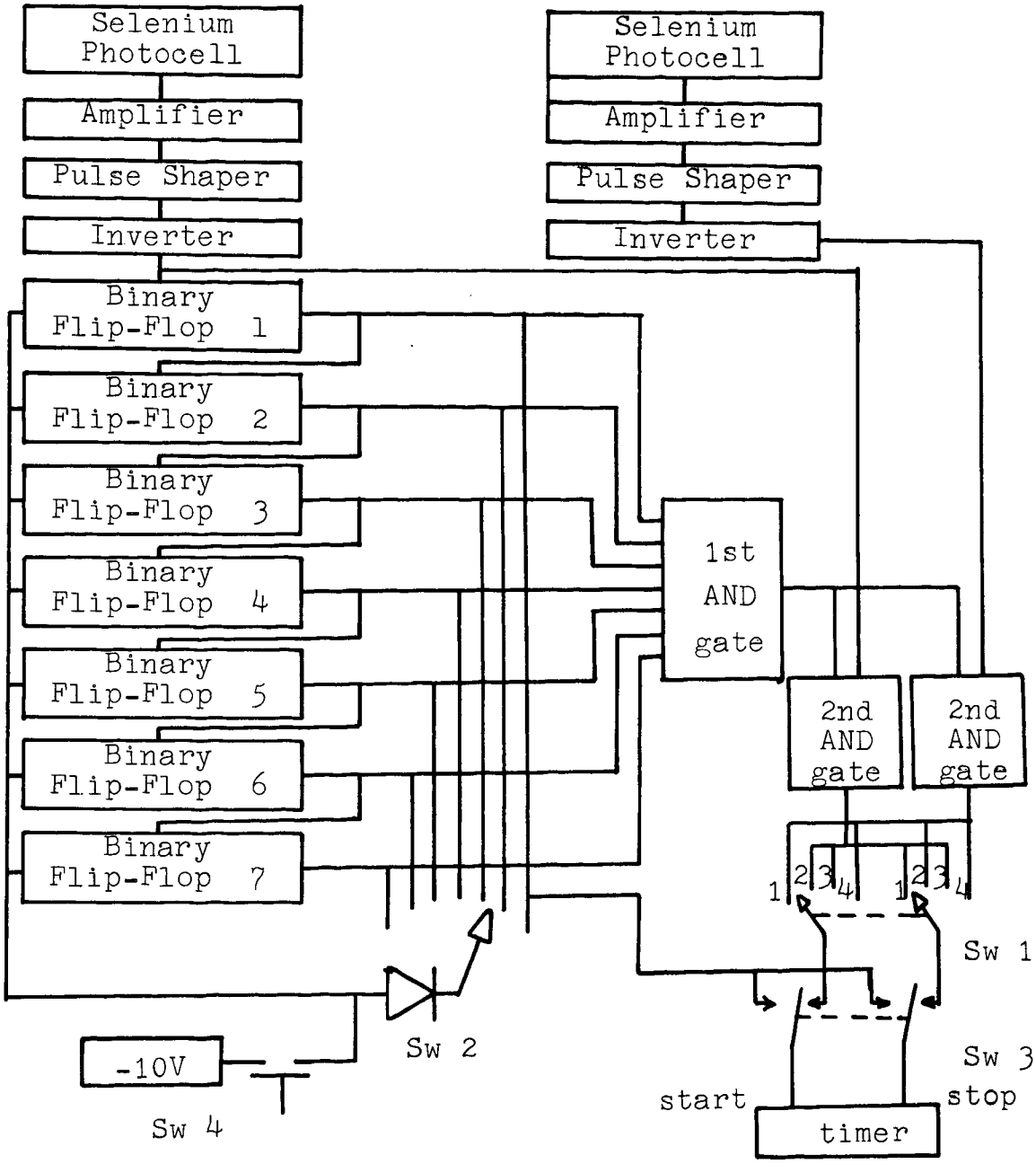

Sw 1 Function Switch

Sw 2 Cycle Switch

Sw 3 Period Switch

Sw 4 Reset Switch

Figure 14. Block Diagram of Detection System

APPENDIX B

Sample Moment of Inertia Calculation, Magnet Assembly

The magnet used to fasten the mirrors to the torque rod has the geometry of a square box with a hole through the center. The moment of inertia is that of the box less the moment of inertia of a cylinder the size of the hole and with the same density as the magnet.

The moment of inertia of a square box of side a and height h is

$$I = \int_{-\frac{h}{2}}^{\frac{h}{2}} \int_{-\frac{a}{2}}^{\frac{a}{2}} \int_{-\frac{a}{2}}^{\frac{a}{2}} (x^2 + y^2)\, \rho \, dx \, dy \, dz \qquad (24)$$

where ρ is the density and when the box is centered on the origin with its equal dimensions in the x and y directions. After integration this equation becomes

$$I = \frac{\rho a^4 h}{6} \qquad (25)$$

The moment of inertia of a right circular cylinder of radius R and height h is

$$I = \rho \int_{-\frac{h}{2}}^{\frac{h}{2}} \int_{0}^{2\pi} \int_{0}^{R} r^2 \, r \, dr \, d\theta \, dz \qquad (26)$$

with the cylinder centered about the origin and with the axis of symmetry coinciding with the z axis. After

integration this becomes

$$I = \frac{\rho R^4 h\pi}{2} . \tag{27}$$

The total moment of inertia of the magnet is the difference

$$I = \frac{\rho a^4 h}{6} - \frac{\rho R^4 h\pi}{2} \tag{28}$$

or

$$I = \frac{\rho h}{2} \left(\frac{a^4}{3} - \pi R^4\right). \tag{29}$$

The density ρ can be replaced by its equivalent M/V where M is the mass of the magnet and V is the volume, i.e., the volume of the box less the volume of the cylinder. This yields

$$I = \left(\frac{M}{6}\right) \frac{a^4 - 3\pi R^4}{a^2 - \pi R^2} \tag{30}$$

or

$$I \simeq \left(\frac{M}{6}\right) \frac{(a^2 + 3R^2)(a^2 - \pi R^2)}{a^2 - \pi R^2} \tag{31}$$

and

$$I \simeq \frac{M}{6} (a^2 + 3R^2). \tag{32}$$

APPENDIX C

Error Analysis of the Theoretical Calculation of the Moment of Inertia

A quantity calculated from physical measurements is always subject to some error because of the error in the basic measurements. Calculus provides a method of evaluating this resultant error from a knowledge or estimate of the error in measurement.

If F is a function of the quantities X_i, i=1,2,...n, the ith quantity in error by an amount dX_i, then the error in F due to the error in X_i is

$$\Delta_i F = \frac{\partial F}{\partial X_i} dX_i \tag{33}$$

hence the maximum total resultant error in F is

$$\Delta F = \sum_{i=1}^{n} \frac{\partial F}{\partial X_i} dX_i \ . \tag{34}$$

As an example, the calculated maximum error due to errors in dimensioning are given below for the moment of inertia of the magnet used to fasten the mirrors to the torque rod. As shown in Appendix B, the moment of inertia is given by the equation (32),

$$I = \frac{M}{6} (A^2 + 3R^2). \tag{32}$$

The three measured quantities M, A and R were:

$$M = 12.290 \pm .001 \text{ gm.}$$

$$A = 1.90 \pm .03 \text{ cm.}$$

$$R = 0.40 \pm .03 \text{ cm.}$$

Using equation (34), one obtains

$$\Delta I = \frac{\partial I}{\partial M} dM + \frac{\partial I}{\partial A} dA + \frac{\partial I}{\partial R} dR \qquad (35)$$

or

$$\Delta I = \frac{1}{6}(A^2 + 3R^2)dM + \frac{1}{3}MA\, dA + MR\, dR \qquad (36)$$

and

$$\Delta I = 0.00068 + 0.233 + 0.147$$

$$= 0.381 \text{ gm.cm}^2.$$

The greatest uncertainty in the moment of inertia calculations is in the threaded cross arm where it was necessary to assume an effective diameter for the threaded portion. At low values for the moment of inertia this is the largest single source of error. The error estimate for each component shown in Table III was calculated using the calculus method described above.

TABLE III

Moment of Inertia Error Estimate

Component	absolute error ($gm.cm.^2$)
Torque rod	0.04
Cross arm and collar	61.86
Magnet	0.38
Mirrors (2)	0.82
Weights (2)	0.40
Weight locks (2)	0.40
Pin vises (2)	0.0
Weight offset	$2.23 + 0.13n + 0.078n^2$
Total	$66.13 + 0.13n + 0.078n^2$

BIBLIOGRAPHY

1. Day, D. E. and Rindone, G. E. (1961) "Internal Friction of Progressively Crystallized Glasses" J. Am. Cer. Soc. 44, (4), 161.

2. Zener, C. (1948) Elasticity and Anelasticity of Metals, University of Chicago Press, 170 pp.

3. Entwistle, K. M. (1962) "The Internal Friction of Metals" Met. Rev. 7, (26), 175.

4. Ke, T. S. (1947) "Experimental Evidence of the Viscous Behavior of Grain Boundaries in Metals" Phys. Rev. 71, 533.

5. Ke, T. S. (1948) "Anelastic Properties of Iron" American Institute of Mining and Metallurgical Engineers Technical Publication No. 2370.

6. Klien, M. J. (1964) "Internal Friction Near the Neel Temperature of Chromium" Phil. Mag. 10, (103), 1.

7. McCrum, N. G. (1961) "Internal Friction in Polyoxymethylene" J. Polymer Sci. 54, 561.

8. Eby, R. K. and Wilson, F. C. (1962) "Relaxations in Copolymers of Tetrafluoroethylene and Hexafluoropropylene" J. App. Phy. 33, (10), 2951.

9. Guye, C. E. and Vasileff, S. (1914) Arch. Sci. Phys. Nat., 3, 214.

10. DeMorton, M. C., Lott, S. A. and Stainsby, D. F. (1963) "Measurement of Internal Friction by Velocity Observations of Torsional Oscillations" J. Sci. Instrum., 40, 441.

11. Sauer, J. A. (1954) "Energy Dissipation in Vibrating Solids" The Virginia Journal of Science, 5, (3), 144.

12. Forry, K. E. (1957) "Two Peaks in the Internal Friction as a Function of Temperature in Some Soda Silicate Glasses", J. Am. Cer. Soc., 40, 90.

13. Rotger, H. (1958) "The Elastic Relaxation Behavior of Simple and Mixed Alkali Silicates and Borates" Glastechn. Ber., 31, 54.

14. Douglas, R. W. and Mohyuddin, I. (1960) "Some Observations of the Anelasticity of Glasses", Phys. and Chem. of Glass, 1, (3), 71.

15. Day, D. E. and Rindone, G. E. (1962) "Properties of Soda Aluminosilicate Glasses: II, Internal Friction" J. Am. Cer. Soc. 45, (10) 496.

16. McCormick, J. M. (1955) "Apparatus for Measurement of Viscoelastic Properties of Glass" J. Am. Cer. Soc. 38, (8), 288.

17. Blum, S. L. (1955) "Some Physical Factors Affecting The Internal Damping of Glass" J. Am. Cer. Soc. 38, 205.

18. Klein, M. J. (1964) "Internal Friction Near the Neel Temperature of Chromium" Metal Science Group, Battelle Memorial Institute, Columbus, Ohio.

19. Horton, F. (1904) "On the Modulus of Rigidity of Quartz Fibers and Its Temperature Coefficients" Trans. Roy. Soc. (London), A204, 407.

20. Spinner, S. (1956) "Elastic Moduli of Glasses at Elevated Temperatures by a Dynamic Method" J. Am. Cer. Soc. 39, 113.

VITA

Thomas Frederick Miller was born in Farmington, Missouri, on July 23, 1940. He received his elementary education through the Saint Louis City Public School System. His preparatory education was received from Central High School, Saint Louis, Missouri from which he graduated January 1959.

He enrolled in the Missouri School of Mines and Metallurgy in February 1959 and received his Bachelor of Science in Physics May 1963. In June 1963 he entered the Graduate School of the University of Missouri at Rolla.